ENGINEERING RESEARCH INSTITUTE
UNIVERSITY OF MICHIGAN
ANN ARBOR

BIMONTHLY PROGRESS REPORT NO. III
THERMAL-SHOCK INVESTIGATION

BY

P. F. CHENEA

A. R. BOBROWSKY

Project M949

WRIGHT AIR DEVELOPMENT CENTER
CONTRACT AF 33(038)-21254, E.O. NO. 605-227-SR-3a

November, 1951

BIMONTHLY PROGRESS REPORT NO. III

THERMAL-SHOCK INVESTIGATION

OBJECT

The object of this research is to evaluate optimum design of test specimens and criteria which will permit correlation of thermal-shock data with performance of the material in the form of turbine buckets.

SUMMARY

A number of new conditions of test were examined including:

a) location of cooling-air nozzle;
b) larger diameter of thermocouple hole; and
c) circular cross section of specimen.

Reproducibility tests were begun on type 347 stainless-steel specimens with no axial load. Specimens of Inconel and Haynes-Stellite 21 alloy have been examined, in addition to type 304 and 347 stainless steels.

A dimensional analysis was made of temperature and stress conditions for different materials. An analysis was made of the unequal distribution of electric current in the specimen due to skin effect. It is believed that this effect is negligible.

INTRODUCTION

The previous progress report indicated that cracking by slow heating and rapid air cooling was practicable on at least two shapes of specimens in both as-rolled and stress-relieved conditions. It appeared desirable at this point to begin a study of reproducibility of results.

APPARATUS

General

The apparatus now employed is shown in Fig. 1. The components may be grouped in the following categories:

a) temperature control and measurement;
b) heating control and supply;
c) cooling control and supply; and
d) specimen holder.

Many general features of the specimen shape have been sufficiently studied to warrant some standardization for the immediate future.

Specimen Shape

The specimen shape is shown in Fig. 2. A bar 1/2 inch in diameter and 7 inches long is held in specimen grips at each end. Water-cooled copper electrodes are clamped on the specimen next to the grips near the central test section. The test section is an equilateral triangle, rounded into the circular bar by fillets of 1/2- to 1-inch radius. The edges of the triangle are finished to widths of 0.015 to 0.030 inch.

The thermocouple hole is symmetrically located. Its diameter is either 1/4 or 1/8 inch. Guard rings were previously employed to make the temperature more uniform along the length of the test section. Their use has been discontinued because the increase in uniformity of temperature was not sufficiently great.

A specimen of round cross section of type 347 stainless steel was tested, but grooves appeared instead of cracks during the test (see Fig. 3). Further study of round specimens will be deferred until the grooving type of failure is better understood or until specimens of this type can be made to yield sharp thermal cracks of the type more characteristic of bucket cracks.

Temperature Control and Measurement

A Chromel-Alumel thermocouple is inserted through the specimen grips into the central hole in the specimen. The thermocouple is connected to a galvanometer-type indicator that also serves to cut off the heating current when the upper cycle temperature is reached.

The temperature indicated by the instrument is in error at both the uppermost and lowermost temperatures because

a) the instrument possesses inertia;
b) the instrument possesses viscous drag;
c) the thermocouple has heat capacity; and
d) the position of the thermocouple with respect to the test section of the specimen varies due to the specimen distortion during heating and cooling.

These effects set a lower bound on the heating time for a given accuracy. The heating time, of course, depends upon the heating rate and the upper and lower temperature.

For instance, with a 30-second heating cycle and a 4-second cooling period, the temperature indicator overshoots the upper present temperature by about 30°F. This overshoot can be decreased by using still longer heating times. Longer heating times give rise to longer test periods per specimen so that a compromise must be set that minimizes overshoot yet permits a reasonable duration of test. Actual heating rates have consequently been set at a level that yields about 45- to 60-second heating times for a specimen temperature of 1600°F. With this heating time the overshoot is estimated not to exceed 10°F.

With test conditions adjusted to yield cracks within the range of about 2000 to 5000 cycles, the actual specimen test time does not exceed about 80 hours.

Heating Control and Supply

The 60-cycle a-c current is stepped down by a variable transformer. The variable feature is required because

a) electrical resistances of different specimens are different; and
b) mean electrical resistance over a test cycle rises until cycle temperatures have reached equilibrium values (after about 10 to 15 cycles from a cold start).

A power transformer capable of handling the large specimen heating current is used to step down the voltage to the final value. Electrodes are water-cooled and soldered to the water tubes to insure good heat transfer. A safety timer is adjusted so that the apparatus is shut down if the time for any one cycle exceeds the time of previous cycles by about 15 seconds. Heating voltage and current are indicated by suitable meters.

Cooling Control and Supply

An air blast of 4-second duration cools the specimen when maximum cycle temperature has been reached. The nozzle provides a narrow jet of air at high speed and flow rate approximately uniformly along the one-inch test section. An electrically-operated valve starts and stops the air flow. The nozzle is rigidly held by supports so that the reaction force of the jet does not sensibly disturb the alignment either during the cooling portion of the cycle or from cycle to cycle.

The position of the air jet relative to the specimen is still under study. In order to minimize setup difficulties, the nozzle has recently been set further from the specimen than in early tests, and directed normally to the flat side of the triangle at the edge. With this setup there has been observed an increase in a type of grooving failure on the flat side of the specimen (as well as on the surface of a round specimen) that does not resemble thermal cracks seen in earlier specimens nor on turbine buckets and nozzle vanes (see Fig. 3). While these grooves ultimately form cracks that proceed across the test edge, it is not known whether these cracks are analogous to cracks observed in previous tests where no grooving was present.

Specimen Holder

The specimen bends a large amount during the cooling portion of the test cycle. It was consequently necessary to support the specimen holders so that the specimen would be returned to its proper position by the end of the heating period. This support was made of laboratory clamps and bars such that the air blast itself did not greatly deflect the specimen. All restraining members were sufficiently long that deflections were always in the elastic range of the supporting structure. Electrical leads are flexible.

Specimen Machining

The drilling of a small-diameter thermocouple hole has proved to be troublesome. A 1/8-inch hole was originally used, but it was proposed that a 1/4-inch hole might be satisfactory for test purposes and at the same time reduce machining difficulties. It was found, however, that a 1/4-inch hole yielded anomalous results in several tests because of the small wall thickness at the area of nearest approach of the hole to the wall. For example, Fig. 4a shows a photograph of a specimen of Haynes-Stellite 21 alloy in which the first crack appeared at the thin wall.

Even with a 1/8-inch hole, drill runout can thin the wall excessively. For example, Fig. 4b shows the breaking-out of the thin wall at the uncooled back side of a type 347 stainless-steel specimen due to repeated stressing during the cycling process. As a result of these and similar experiences, the original procedure of drilling a 1/4-inch pilot hole and continuing into the test section with a 1/8-inch hole will be resumed.

DIMENSIONAL ANALYSIS

General

The object of this section is the determination of the dimensionless parameters that are associated with the distribution of temperature and stress in an isotropic homogeneous elastic body whose physical properties at any temperature may be expressed by constant average values over the duration of the test.

The general equations involved in this study are the heat-conduction equation and the equations of elasticity.

Temperature-Distribution Parameters

For the heating portion of the test cycle, the temperature distribution is given by Eq 1 taken from Ref. 1.

$$\rho c \frac{\partial \Theta}{\partial t} = k \, \Delta^2 \, \Theta + q \quad , \tag{1}$$

where ρ = mass density;
c = specific heat per unit mass;
Θ = absolute temperature;
t = time;
k = thermal conductivity;
q = heat supplied per unit volume per unit time; and
Δ^2 = Laplacian operator.

In the following analysis it is assumed that the physical properties of the materials may be represented by uniform mean values over the applicable temperature range.

Heat is supplied by electrical-resistance heating.

$$q = i^2 r \quad , \tag{2}$$

where i = current density; and
r = electrical resistivity of the specimen material.

For a specimen whose cross section normal to the direction of current flow does not vary abruptly, the heat supplied may be expressed in terms of electrical variables and geometry:

$$q = \frac{I^2 r}{A^2} = \frac{E^2 r}{A^2 (R + \frac{L}{A} r)^2} , \qquad (3)$$

where I = electrical current;
A = cross-sectional area of specimen;
E = line voltage;
R = external circuit resistance; and
L = length of specimen.

Eq 3 may be cast in dimensionless form by defining the following variables and substituting them in (3):

$$\left.\begin{aligned} x_i' &= x_i/D \\ t' &= t/T \\ \theta' &= \theta/\Theta \end{aligned}\right\} \qquad (4)$$

where x_i', t', θ' = dimensionless variables;
x_i = any linear dimension of the specimen;
D = characteristic length;
T = characteristic time; and
Θ = characteristic temperature.

Equation 1 then yields the following dimensionless parameters by the usual processes of dimensional analysis:

$$\pi_1 = \frac{kT}{\rho c D^2} \qquad \text{(Fourier number)}$$

$$\left.\begin{aligned} \pi_2 &= RD/r \\ \pi_3 &= \frac{E^2 T}{\rho c r \Theta D^2} \end{aligned}\right\} \quad \pi_{2,3} = \frac{E^2 T}{\rho c R \Theta D^3}$$

Heat is lost from the surface of the specimen due to convection, conduction, and radiation. At the cooled grips, conduction is the primary process of heat transfer, while at the test section, heat transfer takes place chiefly by convection and radiation. If the specimen grips are assumed to be constant in temperature, the boundary condition at the cooled ends is

$$\theta = \theta_o = \Theta\, \theta_o' \quad , \tag{5}$$

where θ_o = absolute temperature of grips; and

θ_o' = dimensionless temperature of grips.

Hence $\Pi_4 = \theta_o'$.

At the portions of the specimen exposed to the surrounding air, the boundary condition at the surface may be expressed during the heating cycle as

$$k \frac{\partial \theta}{\partial n} + \sigma \varepsilon (\theta^4 - \theta_1^4) + h(\theta - \theta_2) = 0 \quad , \tag{6}$$

where n = unit normal;

σ = Stefan-Boltzmann constant;

ε = emissivity;

θ_1 = mean absolute temperature of surroundings;

h = heat transfer coefficient for natural convection; and

θ_2 = absolute mean temperature of surrounding air.

This equation yields the following dimensionless parameters:

$$\Pi_5 = \frac{\sigma \Theta^3 D}{k}$$

$$\Pi_6 = hD/k \quad \text{(Biot number)}$$

$$\Pi_7 = \varepsilon$$

$$\theta_1' = \theta_1/\Theta$$

$$\theta_2' = \theta_2/\Theta$$

The initial condition, that is, the temperature level and distribution at the start of the heating cycle, is essentially

$$\theta(x,y,z,) = \theta_3(x,y,z) = \Theta\theta_3'(x,y,z) \quad ,$$

where $\theta_3(x,y,z)$ = temperature of the specimen immediately after cooling by air blast; and

$\theta_3'(x,y,z)$ = dimensionless temperature of the specimen immediately after cooling by air blast.

For the heating period, the temperature at a point in the specimen at any time may be expressed as

$$\theta = \Theta \Phi \left[\left(\frac{kT}{\rho c D^2}\right), \left(\frac{R_D}{r}\right), \left(\frac{E^2 T}{\rho c r \Theta D^2}\right) \left(\frac{\sigma \Theta D}{k}\right), \left(\frac{hD}{k}\right), \varepsilon, \theta_i', x_i', t' \right] \qquad (7)$$

where Φ = a function, and

θ_i' = dimensionless temperatures.

For the cooling period the parameters are the same as for the heating period except that π_6 is replaced by

$$\pi_8 = \left(\frac{fD}{k}\right),$$

where f is the heat-transfer coefficient for forced convection; and the initial condition becomes

$$\theta(x,y,z) = \theta_4(x,y,z) = \Theta \theta_4'(x,y,z) \quad , \qquad (8)$$

where $\theta_4(x,y,z)$ = temperature distribution in specimen immediately after heating ceases, and

$\theta_4'(x,y,z)$ = distribution of dimensionless temperature in specimen immediately after heating ceases.

The question arises as to whether there are sufficient parameters available to permit their adjustment in such manner as to achieve identical dimensionless-temperature distributions in specimens of different materials. The applicable material properties that are subject to variation among materials and the parameters that may be adjusted are shown in the table below.

	Material Property	Adjustable Parameter
k	thermal conductivity	D characteristic length
(ρc)	heat capacity per unit volume	Θ characteristic temperature
h	coefficient of heat transfer for natural convection	T characteristic time
ε	emissivity	E line voltage
r	electrical resistivity	R external resistance

In a theoretical sense, the dimensionless temperature distribution could be maintained identical among specimens of different materials at any given dimensionless time by the following adjustments (assuming negligible variation of emissivity among specimens): The x_i' will be constant with geometrically similar specimens, and the θ_i' can be made constant by suitably adjusting the boundary conditions. Both line voltage, E, and the circuit resistance, R, are available to compensate for (ρc) in $\pi_{2,3}$; the characteristic time, T, is available to compensate for ($k/\rho c$) in π_1; the characteristic specimen dimension, D, is available to compensate for (h/k) in π_6;

and the characteristic temperature may be varied to compensate for k in Π_5. Π_8 is best maintained constant by adjusting the air blast. ϵ cannot be compensated since it is itself dimensionless. In a practical sense the feasibility and desirability of varying T, which is a function of cycle time; D, the specimen dimension; Θ, the characteristic temperature; and f, the forced-convection heat-transfer coefficient, are open to question.

The determination of the actual variation of temperature among specimens of different materials must await the numerical solution of this rather complicated boundary-value problem. It is not felt that the numerical analysis is necessary at this time. Since the actual functional relationship is not known, a statement of the ranges of the variables involved is not given at this time.

Stress-Distribution Parameters

The variation of stress in a specimen due to nonuniform temperature may be examined by the theory of elasticity. Plastic deformation is also present, but as a first approximation, only an elastic stress distribution will be considered.

For static equilibrium in a rectangular Cartesian coordinate system:

$$\left.\begin{aligned} \frac{\partial s_{xx}}{\partial x} + \frac{\partial s_{xy}}{\partial y} + \frac{\partial s_{xz}}{\partial z} - 3\alpha K \frac{\partial \Theta}{\partial x} &= 0 \\ \frac{\partial s_{xy}}{\partial x} + \frac{\partial s_{yy}}{\partial y} + \frac{\partial s_{yz}}{\partial z} - 3\alpha K \frac{\partial \Theta}{\partial y} &= 0 \\ \frac{\partial s_{xz}}{\partial x} + \frac{\partial s_{yz}}{\partial y} + \frac{\partial s_{zz}}{\partial z} - 3\alpha K \frac{\partial \Theta}{\partial z} &= 0 \end{aligned}\right\} \qquad (9)$$

where s_{xx}, s_{yy}, s_{zz} = components of direct stress;
s_{xy}, s_{yz}, s_{xz} = components of shear stress;
x, y, z = coordinates;
α = coefficient of linear thermal expansion;
K = bulk modulus of elasticity; and
Θ = absolute temperature.

The stress-strain relations for an elastic material are

$$\begin{aligned} s_{xx} &= 3K\,(e_{xx} - \alpha\Theta) \\ s_{yy} &= 3K\,(e_{yy} - \alpha\Theta) \\ s_{zz} &= 3K\,(e_{zz} - \alpha\Theta) \end{aligned} \qquad (10)$$

$$\frac{s_{xy}}{e_{xy}} = \frac{s_{yz}}{e_{yz}} = \frac{s_{xz}}{e_{xz}} = 2G \tag{10}$$

where e_{xx}, e_{yy}, e_{zz} = extensional strain;
e_{xy}, e_{yz}, e_{xz} = shear strain; and
G = shear modulus of elasticity.

The equations of compatibility of stress or strain do not introduce any additional variables.

In the interests of brevity of notation, coordinates and stresses in general will be represented by x_u and s_{uv}. The following variables may be introduced:

$$s_{uv}' = s_{uv}/3K$$
$$x_u' = x_u/3K \quad . \tag{11}$$

After substituting Eq 11 in Eqs 9 and 10, and performing dimensional analysis, new dimensionless terms appear:

$$(\alpha\Theta) = \pi_9$$
$$\left(\frac{2G}{3K}\right) = \left(\frac{1 - 2\mu}{1 + \mu}\right) = \pi_{10} \quad ,$$

where μ = Poisson's ratio.

A reduced stress may be set up to characterize the stress distribution:

$$s_{uv}(\text{reduced}) = s_{uv}/3K\alpha\Theta \quad .$$

Theoretically, $(\alpha\Theta)$ could be maintained constant for different materials by varying Θ, the characteristic temperature. π_{10}, of course, would have to vary unaffected by any parameters other than μ.

UNEQUAL DISTRIBUTION OF ELECTRIC CURRENT

General

The heating of the specimen is accomplished by electrical-resistance methods. Since a large conductor is used, skin effect may be expected to be present. The purpose of this section is to estimate the magnitude of this effect.

Skin Effect

It is not immediately obvious that the assumption of uniform current density over the cross section of the specimen is valid when alternating current is used for heating. A magnetic field is established both exterior to and inside a conductor when current flows. The equipotentials of the magnetic field, in the case of a long cylindrical conductor, are concentric cylinders whose generators are parallel to the axis of the conductor. The magnetic field varies with time, since the current varies with time, and may consequently be characterized by a system of expanding and contracting concentric cylinders (see Refs. 2 and 3).

An electromotive force is induced by the alternating flux in each of the elementary axial filaments of which the conductor may be considered to be composed. This induced electromotive force is due partly to the external field and partly to the internal field. The field external to the conductor encloses all filaments, whereas each internal cylinder encloses only the filaments within it. Hence the external field induces the same emf in all filaments while the internal field induces a greater emf in the filaments nearer the axis. Kirchhoff's laws require that the sum of the induced emf and the potential drop due to resistance be the same in all filaments. The current must distribute itself, consequently, with higher current density nearer the surface of the conductor. This variation in the current density is called skin effect.

Skin effect depends on the frequency of the applied emf, the cross-sectional area of the specimen, electrical conductivity, and magnetic permeability of the conductor. The effect is increased by an increase in these parameters. It decreases with increasing temperature because conductivity decreases with increasing temperature for the alloys of interest in the present investigation.

As a first approximation, let the cross section of the conductor be circular, and let end effects be neglected. It is shown in the references cited that skin effect is described by the following equation:

$$i_w = i_a \frac{J_o(j^{3/2}\,Yw)}{J_o(j^{3/2}\,Ya)} ,$$

where i_w = current density at a distance w from the axis of the conductor;
i_a = current density at the surface of a conductor of radius a;
J_o = Bessel function of index zero;
j = square root of minus one; and

$$Y = \sqrt{\frac{4\pi^2\mu\omega}{r}} ,$$

where μ = magnetic permeability of the conductor;
ω = circular frequency; and
r = resistivity of the conductor.

At a frequency of 60 cycles per second, for a magnetic permeability of unity, and for a resistivity of 72 microhm-cm, the minimum radius of a conductor having a skin effect of 0.1 per cent is about 3/4 inch, where skin effect is defined as the ratio $(i_a - i_w)/i_a$. Hence skin effect may be expected to be negligible in these tests provided specimen size is not increased.

RESULTS AND DISCUSSION

Experimental

A log of test results is appended. The materials used to date are type 304 and 347 stainless steels, Inconel, and Haynes-Stellite 21 alloy. The chief conclusions to be drawn from the log are:

a) Specimens of triangular and square cross section are most suitable for testing.
b) The formation of large grooves precedes cracking under certain circumstances.
c) The nature and incidence of cracking is sensitive to location of the air jet.
d) Thermal cracking can be induced in several alloys by repeated air cooling of specimens under no mechanical load.

The type of crack formed in stainless steels is readily distinguished from cracks produced by mechanical means alone. Fig. 5a shows the appearance of cracks produced by tearing at the end of a creep-rupture test; these cracks are essentially of mechanical origin. It may be noted that a pulling-apart has occurred and that opposing faces of cracks mate reasonably well if brought together. Fig. 5b is a cross section of a thermal crack in type 304 stainless steel. It may be noted that the sides of the crack do not mate, either because of plastic deformation on repeated compression or due to corrosion. The crack is more smooth-sided than the fracture cracks and changes rapidly in width near the closed end. It is too early to state definitely that these differences are always present and in all alloys. Investigation of cracks in the vicinity of failed turbine buckets, however, may prove of interest in determining whether the features of these cracks are more nearly similar to those obtained in these tests by thermal cracking or to mechanically-induced cracks.

The probability that deterioration is progressive was mentioned in the previous progress report. This deterioration could be due to temperature, fatigue, or stress-rupture. In order to determine whether fatigue damage will hasten thermal cracking, it is planned to test specimens that have been subjected to some cycles of repeated stress at a level above the endurance limit or at a stress at which it is known that fatigue failure occurs. The log consequently shows entries of fatigue specimens used to estiblish values of stress at which fatigue damage can be obtained.

Theoretical

A complete analysis of thermal cracking would entail:

a) determination of temperature, stress, and strain distribution in the test specimen;
b) determination of a criterion for tensile failure in terms of deterioration caused by combined stress-rupture and fatigue history at varying temperatures; and
c) correlation of stress, strain, and temperature history as determined in part a) with the criterion of failure in part b).

The present analysis is a portion of part a) above in that the parameters governing temperature and elastic stress have been set up under certain simplifying assumptions.

It can be stated that materials with approximately the same values of dimensionless Pi terms will set up about the same magnitude and distribution of stresses in test specimens of different sizes but of geometrically similar shape, assuming that the heat-transfer coefficients for forced convection are not affected by change in specimen size and assuming that thermal boundary conditions are adjusted to maintain similarity.

The adjustment of parameters so that Pi terms may be held constant is a difficult procedure. Variation of external thermal conditions would involve considerable additional apparatus. Variation of cycle time would introduce a variable ratio of time at temperature to number of cycles per unit time. Moreover actual values of parameters set up in the foregoing analysis such as emissivity, Poisson's ratio, and ratio of thermal conductivity to coefficient of heat transfer through surface film are not completely known for the temperature range of interest. It is consequently indicated that it is not feasible at this time to attempt to impose identical stresses in different alloys by variation of test conditions. The magnitude of departure from identical stress conditions depends on the functional relationship of these parameters, and this relationship depends on the specimen shape used. The solutions of the equations for thermal stress consequently involves a lengthy numerical procedure for each shape being investigated. It may be concluded that a solution for the temperature and stress distribution is not easily attainable at present.

The effect of an electric current on temperature distribution is probably not more than about 1 per cent. Inasmuch as this effect is not present during the cooling portion of the test cycle, the only influence of the effect is to alter the temperature distribution at the start of the cooling period. The rapid cooling of the specimen is believed to be more responsible for thermal cracking than the slow heating for specimens used in this test. It may be concluded that the small variation in initial temperature has little effect on temperature distribution during the cooling period within a very short time after the cooling begins.

SUMMARY OF RESULTS

1. Grooving was found to precede cracking in certain tests where the location of the air jet was unfavorable.

2. The effect of an electric current on temperature is thought to be less than 1 per cent.

3. A number of parameters that govern cracking have been examined. Data are lacking on many physical properties embodied in these parameters.

REFERENCES

1. Carslaw, H. S., and Jaeger, J. C.: Conduction of Heat in Solids. Oxford. 1947. Page 9.

2. Wall, T. F.: Principles of Electrical Engineering. Chemical Publishing Company. 1947. Pages 433 ff.

3. Pender, H., and Del Mar, W. A.: Electrical Engineer's Handbook. Wiley. 3rd ed. 1947. Pages 3 - 21, ff.

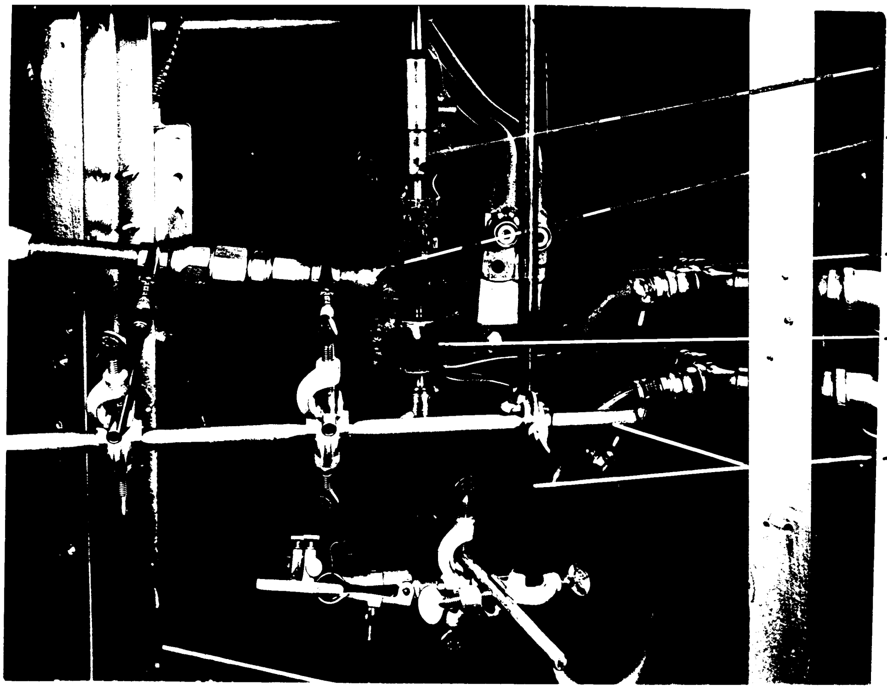

a) Cooling nozzle directed at specimen

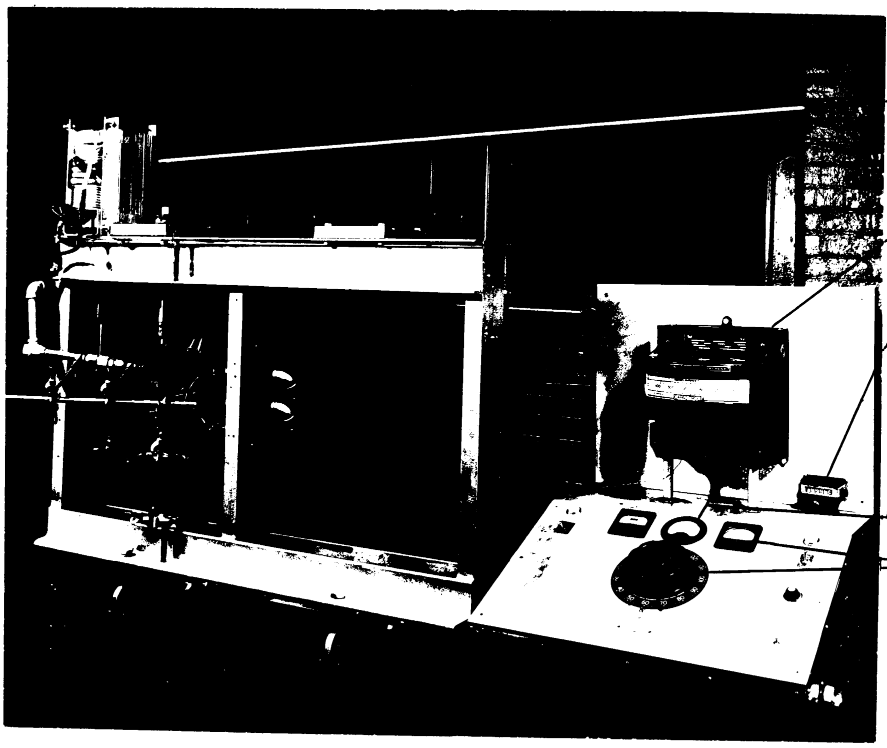

b) Test frame and control panel

Fig. 1. Test Setup

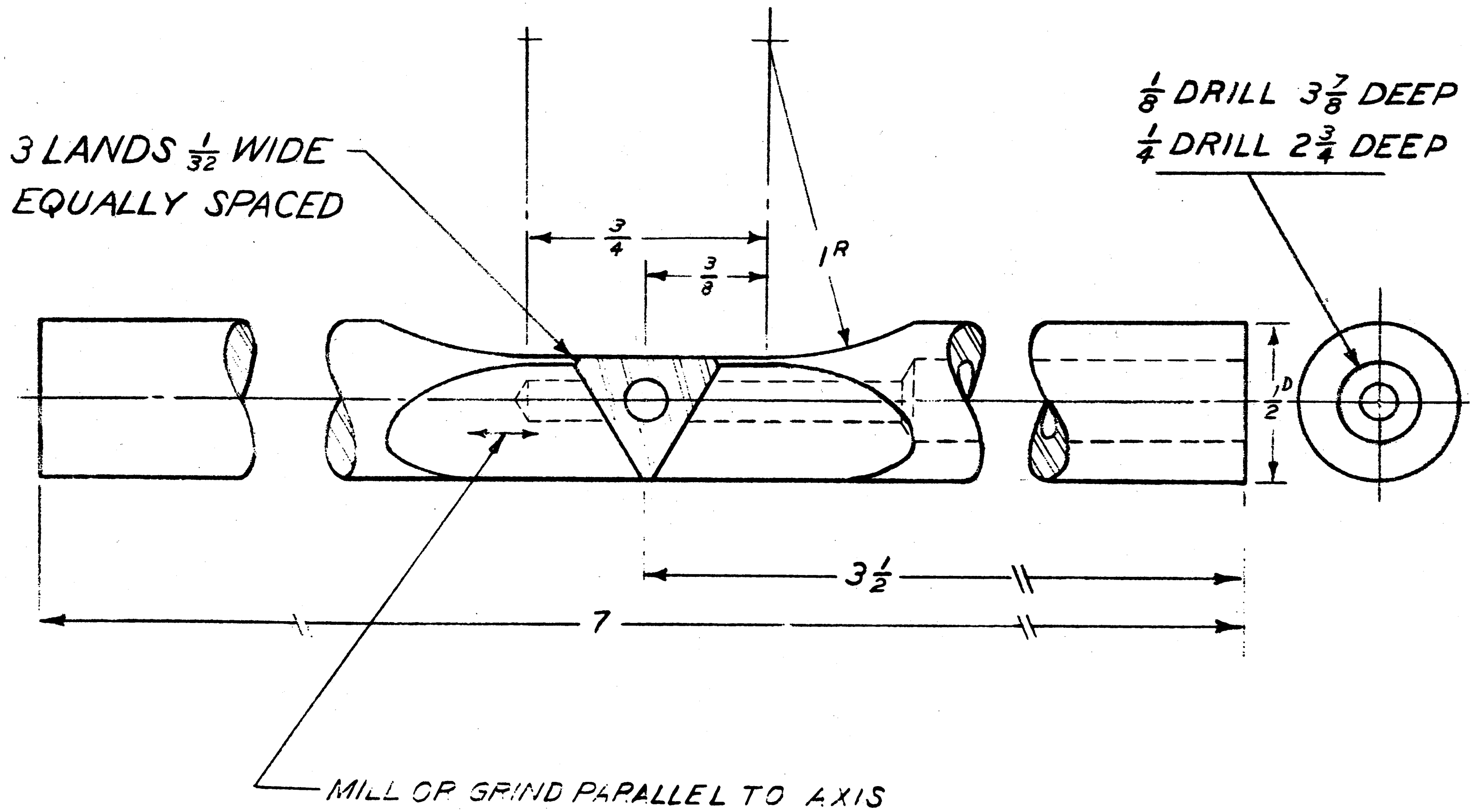

Fig. 2 Thermal-shock Specimen

Fig. 3. Thermal-shock specimen of round cross section after test showing grooves. Material-type 347 stainless steel. 4X.

a) Thermal-shock specimen of Haynes-Stellite 21 alloy. Specimen broken apart after test showing crack formed between surface and central hole of 1/4-inch diameter.

b) Thermal-shock specimen of type 347 stainless steel of triangular cross section showing breaking out of uncooled metal at back of specimen between surface and central hole of 1/8-inch diameter at area where drill run-out has been excessive.

Fig. 4. Anomalous results in thermal-shock specimens due to thin wall at thermocouple hole.

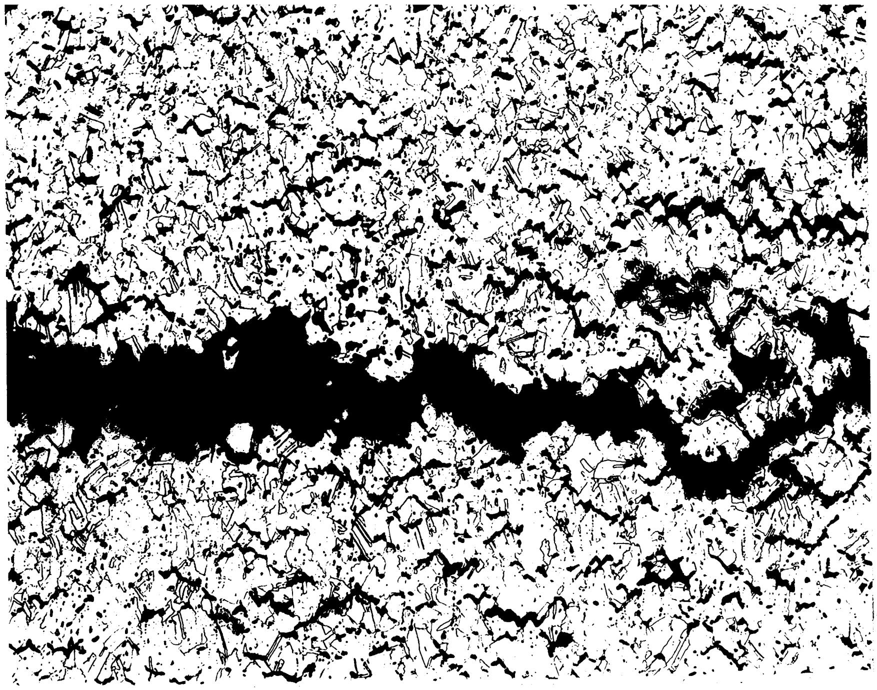

a) Mechanical crack in type 304 stainless steel in vicinity of rupture failure. X100.

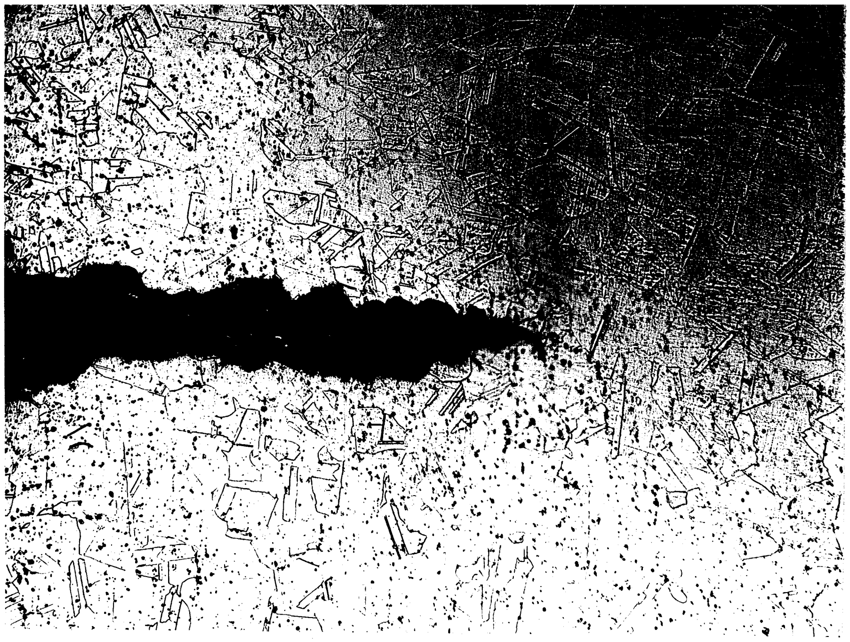

b) Thermal crack in type 304 stainless steel. X100.

Fig. 5. Types of cracks encounted in thermal-shock tests.

19	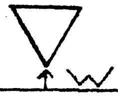	1700/3	530 W	C	
20		1500/3	1000	O	B.T.

Type 347 Stainless Steel

1		1600/4 +10/100	866	C	
2	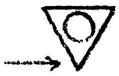	1600/4 +10/100	1147	C	
3		1500/4 +10/100	575	C	B.T.
4a	Fatigue	54 K	5200	F	
4b	Specimens	54 K	10400	F	40.5K 82000
5	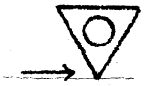	1500/4 +10/100	1326	C	
6	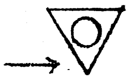	1500/4 +10/100	1990	C	
7	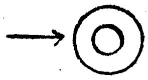	1600/3½ +10/100 to 1800	2700	G	

Inconel

1	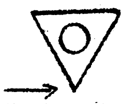	1500/3 +10/100	1450	C	G1150
2	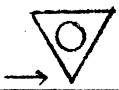	1500/3 +10/100	2730	C	G2310
3		1500/3½ +10/100	428	C	B.T.

I.S. 21 (Vitallium)

1	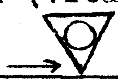	+10/100 1500/3½	1000	C	B.T.

KEY TO LOG

Column (2)	
	Arrow indicates direction and location of cooling jet; cooling medium air unless otherwise stated.
W	Cooling medium -- water.
.045	Width of cooled edge, inches.
Column (3)	
M	Thermal-shock cycle manually controlled.
1500/5	Automatic cycle control; maximum temperature, °F, and length of cooling period, seconds.
P1800	Dead load 1800 pounds.
10/100	Starting with stated maximum temperature, maximum temperature was increased 10°F after each 100 cycles.
40.5K	Reversed-bending (rotating beam) fatigue tests; maximum stress = 40,500 psi.
to 1800	Maximum temperature held constant after 1800°F was reached.
Column (4)	
A	Air cooling for stated number of cycles.
W	Water cooling for stated number of cycles.
no symbol	Air cooling for stated number of cycles.
Column (5)	
O	No failures visible.
F	Fracture.
C	Cracks.
G	Grooves.
Column (6)	
B	Specimen warped due to thermal strains.
A0.14	Area of cross section, square inches.
T300/1600	Heat treated before testing 300 hours at 1600°F
G1500	Grooves first appeared at 1500 cycles.
O.H.	Stated maximum temperature was exceeded due to malfunction of control unit.
B.T.	Broke through to thermocouple hole.
40.5K 82000	Previously subjected to 82,000 cycles at 40,500 psi.

<u>TEST LOG</u>

Specimen Number (1)	Cross Section (2)	Cycle (3)	Number of Cycles (4)	Type of Failure (5)	Remarks (6)
Type 304 Stainless Steel					
1		M	---	0	B
2	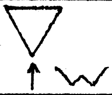	1600/10	4400 A 300 W	C	B
3	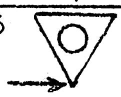	1600/4 +10/100	1783	C	
4a 4b	Fatigue Specimens	40.5 K 40.5 K	3300 2600	F F	
5	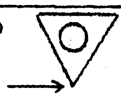	1700/4 1800/4	1100 675	0 C	
6	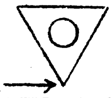	1600/4 1900/4	6240 1240	0 C	G 260
7		1500/5 P600	4130	F	A 0.16
8		1600/5 1800/4	3082 517	0 C	T300/1600
9	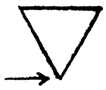	1500/3	5753	0	
10	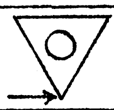	1600/4 1700/4 1800/4	1000 1000 80	0 0 C	
11		1500/5 P1800	1000	F	A 0.132
12		1500/5 P600 P900 P1800	 5000 1200 203	 0 0 F	A 0.133
13	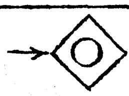	1600/4	1284	C	G1115
14		1500/4	1000	F	O.H.
15		1600/5	1900	C	T300/1600
16	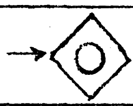	1600/5	409	C	
17		1500/5 P1800	300	F	A 0.14